HHS Public Access

Author manuscript

J Magn Reson Imaging. Author manuscript; available in PMC 2020 February 01.

Published in final edited form as:

J Magn Reson Imaging. 2019 February ; 49(2): 487–498. doi:10.1002/jmri.26218.

Single Scan Quantitative Gradient Recalled Echo MRI for Evaluation of Tissue Damage in Lesions and Normal Appearing Gray and White Matter in Multiple Sclerosis

Biao Xiang, BS[1], **Jie Wen, PhD**[2], **Anne H. Cross, MD**[3], and **Dmitriy A. Yablonskiy, PhD**[2,*]

[1]Department of Chemistry, Washington University, St. Louis, Missouri, USA

[2]Department of Radiology, Washington University, St. Louis, Missouri, USA

[3]Department of Neurology, Washington University, St. Louis, Missouri, USA

Abstract

Background: Multiple sclerosis (MS) is a chronic disease affecting the human central nervous system (CNS) and leading to neurologic disability. Although conventional MRI techniques can readily detect focal white matter (WM) lesions, it remains challenging to quantify tissue damage in normal-appearing gray matter (GM) and WM.

Purpose: To demonstrate that a new MRI biomarker, R2t*, can provide quantitative analysis of tissue damage across the brain in MS patients in a single scan.

Study Type: Prospective.

Subjects: Forty-four MS patients and 19 healthy controls (HC).

Field Strength/Sequence: 3T, quantitative gradient-recalled-echo (qGRE), Magnetization-prepared rapid gradient-echo, fluid-attenuated inversion recovery.

Assessment: Severity of tissue damage was assessed by reduced R2t*. Tissue atrophy was assessed by cortical thickness and cervical spinal cord cross-sectional area (CSA). Multiple Sclerosis Functional Composite was used for clinical assessment.

Results: R2t* in cortical GM was more sensitive to MS damage than cortical atrophy. Using more than two standard deviations (SD) reduction versus age-matched HC as the cutoff, 48% of MS patients showed lower R2t*, versus only 9% with lower cortical thickness. Significant correlations between severities of tissue injury were identified among 1) upper cervical cord and several cortical regions, including motor cortex ($P < 0.001$), and 2) adjacent regions of GM and subcortical WM ($P < 0.001$). R2t*-defined tissue cellular damage in cortical GM was greater relative to adjacent WM. Reductions in cortical R2t* correlated with cognitive impairment ($P < 0.01$). Motor-related clinical signs correlated most with cervical cord CSA ($P < 0.001$).

Data Conclusion: Reductions in R2t* within cortical GM was more sensitive to tissue damage than atrophy, potentially allowing a reduced sample size in clinical trials. R2t* together with

*Address reprint requests to: D.A.Y., Mallinckrodt Institute of Radiology, Washington University, 4525 Scott Ave. Room 3216, St. Louis, MO, 63110. yablonskiyd@wustl.edu

Additional supporting information may be found in the online version of this article.

structural morphometry suggested topographic patterns of regions showing correlated tissue damage throughout the brain and the cervical spinal cord of MS patients.

Multiple sclerosis (MS) is an inflammatory disorder of the central nervous system (CNS) that involves the brain and the spinal cord, often causing neurologic disability. Magnetic resonance imaging (MRI) plays an important role in MS diagnosis,[1] as an endpoint in clinical trials,[2] and as a means to monitor patients.[3] Recent MRI studies have focused on pathological changes in both macroscopic (visible with standard clinical MRI) lesions and normal-appearing tissue (invisible with standard clinical MRI).

Conventional MRI techniques can readily detect focal white matter (WM) lesions. MS plaques are typically bright on T2-weighted (T2W) and FLAIR (fluid attenuated inversion recovery) images and dark on T1-weighted (T1W) images referred to as “gray” or “black holes” that are believed to represent the loss of underlying tissue, especially axons.[4] New approaches, such as phase-sensitive inversion-recovery (PSIR),[5] target MS lesions in gray matter (GM). A limitation of these images is that although they can be used to detect MS lesions, they cannot be used to quantify the severity of tissue destruction. Indeed, if T2W or T1W images indicate that two MS lesions have identical volumes, this does not mean that the two lesions have the same underlying pathology. In addition, neither normal-appearing WM (NAWM), which is often abnormal histologically, nor normal-appearing GM (NAGM) can be identified on T2W or T1W images of MS subjects.[6] In addition to brain pathology, over 90% of MS patients develop spinal-cord lesions, and these cord lesions can greatly impact neurologic disability.[7,8]

Because of this, new approaches utilizing quantitative maps of T2 and T1 relaxation time constants, magnetization transfer ratio (MTR), and diffusion have been proposed[9–13] in addition to standard subjective T2W and T1W images. However, for reasons such as long imaging times, low resolution and low signal-to-noise ratio (SNR), these are not commonly used for MS in clinical practice. Hence, fast, quantitative noninvasive imaging methods that reflect the severity of MS pathology, both in lesions and normalappearing tissue, are needed for prognostication and to monitor patients.[2,14]

Our approach to this problem is based on quantitative measurements of the transverse relaxation properties of the gradient recalled echo (GRE) MRI signal. This quantitative GRE (qGRE) approach,[15] an advanced version of previously developed gradient echo plural contrast imaging (GEPCI) technique,[16] allows estimation of tissue damage in MS lesions and normal-appearing WM and GM. An innovative qGRE method of data analysis[15] allows separation of tissue-cellular- specific (R2t* relaxation rate constant) from blood oxygen level-dependent (BOLD)[17] contributions to the total GRE MRI signal decay rate constant (R2*). Since the BOLD effect causes variations in MRI signal that occur with physiological state-dependent changes in blood flow and/or oxygen consumption, the R2t* values more specifically reflect the tissue- cellular component of R2*. The tissuecellular-specific (R2t*) MRI relaxation parameter depends on the environment of water molecules (the main source of MRI signal): higher concentrations of proteins, lipids, and other constituents of biological tissue and cellular constituents (sources of MRI signal relaxation) leading to higher relaxation rate constants.

The qGRE method that we use also includes acquisition and postprocessing approaches that minimize adverse artifacts related to macroscopic magnetic field inhomogeneities[18] and physiological fluctuations.[19] From these perspectives, the transverse relaxation rate constant R2t* of the GRE signal is a close relative of the transverse relaxation rate R2 of the spin echo signal, but the qGRE approach allows much faster imaging with higher resolution and SNR. Prior studies in autopsied MS CNS tissue demonstrated statistically significant correlations between T2 (1/R2) relaxation time constants and MS pathology both for the spinal cord[20] and brain.[21,22] Due to the similarity between R2 and R2t*, we can conclude that R2t* measurements can serve as a pathological correlate of tissue damage in MS. Besides, measurements in autopsied samples also confirmed the correlation with MS-related tissue damage in GM.[23]

In this study we evaluated the novel MRI biomarker R2t* for quantitative detection of normal-appearing tissue damage in MS patients. We also investigated correlations between loss of tissue quality in different regions of the CNS that could suggest the topographic signatures of tissue damage in MS patients.

Materials and Methods

Subjects

Forty-four MS patients with relapsing remitting (RRMS, $n = 15$), secondary progressive (SPMS, $n = 16$), and primary progressive (PPMS, $n = 13$) MS clinical courses and 19 healthy control (HC) subjects were enrolled, after providing informed consent. HC were recruited to reflect the gender and age distribution of the MS patients. The study was approved by the Institutional Review Board.

Clinical Testing

The Expanded Disability Status Scale (EDSS) standardized neurological examination, 25-foot timed walk (25FTW) assessment of gait, nine-hole peg test (9HPT) assessments of bilateral upper extremity function, and paced auditory serial addition test (PASAT) and symbol digit modalities test (SDMT) assessments of cognitive function were performed on the day of the MRI by examiners blinded to imaging results. For analyses, the 25FTW and 9HPT were converted to Z scores according to the following equations from the Multiple Sclerosis Functional Composite (MSFC)[24]:

$$Z_{25FTW} = (25FTW - 9.5353)/11.4058 \quad (1)$$

$$Z_{9HPT} = (1/9HPT - 0.0439)/0.0101 \quad (2)$$

Image Acquisition

MRI scans were performed with a 3T Trio MRI scanner (Siemens, Erlangen, Germany) using a 32-channel phased-array RF head coil. A previously developed GEPCI protocol[16]

with navigation echo[19] was used to acquire 3D multigradient-echo data with flip angle of 30°, repetition time (TR) = 50 msec, voxel size of 1 × 1 × 2 mm^3 and acquisition time of 11 minutes, 30 seconds. For each phase encoding step, 10 gradient echoes and one navigation echo[19] were collected with first echo time (TE1) = 4 msec and echo spacing ΔTE = 4 msec. Standard clinical MPRAGE[25] images with voxel size 1 × 1 × 1 mm^3 were collected for segmentation purposes and measuring cortical thickness (TH) and spinal cord cross-sectional area (CSA). Fluidattenuated inversion recovery (FLAIR) sequence with voxel size of 1 × 1 × 3 mm^3 was used for outlining WM lesions.

Image Processing and Segmentation

The MRI data were analyzed using the qGRE approach described in a previous study.[15] Details are presented in the Supporting Information. In brief, multichannel data were combined using the GEPCI algorithm[16] and analyzed voxel-wise using the theoretical model of GRE signal relaxation,[26,27] and a set of postprocessing algorithms that minimize adverse artifacts related to macroscopic magnetic field inhomogeneities[18] and physiological fluctuations.[19] This approach allows generation of images and quantitative maps with several contrasts reflecting biological tissue anatomic, microstructural, and functional properties. In this study we used GEPCI T1W images and qGRE R2t* maps. Importantly, all these images are inherently coregistered.

Brain GM and WM segmentation was performed on MPRAGE images using FreeSurfer 5.3.0 (Martinos Center for Biomedical Imaging, MGH/HST, US) with visual inspection of each segmented region of interest (ROI) for accuracy. This resulted in 68 cortical GM and 68 corresponding subcortical WM ROIs (for each ROI, the R2t* and TH in the left and right hemispheres were averaged). A list of ROIs is provided in the Supporting Information. MPRAGE images were coregistered with GEPCI-T1W images (which are intrinsically coregistered with qGRE R2t* maps) using FSL 5.0.0 software (Analysis Group, FMRIB, Oxford, UK). This procedure also coregistered ROIs generated by FreeSurfer to GEPCI-T1W images and R2* maps. To minimize partial volume effects, CSF masks were generated based on the GEPCI T1W images using FSL. Applying regional and CSF masks, median values of R2t* and of cortical GM thickness were calculated for each cortical ROI. 3D MPRAGE data were processed using PropSeg (Spinal Cord Toolbox v. 2.0)[28] to measure the spinal cord CSA. Mean CSA values at the four upper cervical levels were calculated.

Tissue Damage in MS Lesions Based on R2t*

For all subjects, MPRAGE and FLAIR images were registered using FSL and used to obtain WM lesion masks using the “lesion-TOADS” tool[29] in Medical Image Processing, Analysis and Visualization (MIPAV).[30] For each subject, tissue damage within WM MS lesions was quantified in terms of tissue damage load (TDL): a parameter calculated based on the difference between R2t* values of voxel within the lesions and R2t* values of NAWM, similar to a previous R2*-based report[31] (details in the Supporting Information).

Statistical Analysis

Statistical analyses and correlations were performed using MatLab (MathWorks, Natick, MA). Median R2t* values were used to describe each FreeSurfer region in the brain,

because R2t* values in most regions were not normally distributed, and also to minimize edge/partial volume effects and spurious values. Age is known to affect R2t* and reduce cortical thickness[32]; therefore, age-dependent R2t* and cortical thickness values were obtained from the HC cohort of 19 individuals. To account for this effect, the median values of R2t* in each of Free Surfer cortical or subcortical region (n) in the normal HC group were fitted by a linear equation[32]:

$$MedianValue_n = A_n + K_n \cdot (age - < age >) \quad 3$$

where < age > is mean age of HC group. Introducing it in the equation assigns to parameters A_n values corresponding to mean age of participants. This procedure allowed calculation of expected reference regional values for any actual patient age. A similar procedure was used for subcortical WM and FreeSurfer-defined cortical thickness. These calculated values were subtracted from the values of individual HC and MS subjects to generate ΔR2t* and ΔThickness. Spinal cord area was not significantly correlated with age in our data (parameter $K = 0$ in Eq. [3]) and no significant difference of spinal cord area between the male and female groups was found. Thus, the mean CSA value of the entire HC cohort was subtracted from each MS subject CSA values to generate ΔCSA. Due to the small number of male patients (Table 1), gender differences were not taken into account. For spinal cord, no significant correlation was found between spinal cord CSA and age, height, brain size, and disease duration, so these variables were not considered in subsequent data analyses.

To explore topographic signatures of tissue damage in NAGM, Person's correlation analysis was performed between ΔR2t* of each cortical region (n) and ΔR2t* of the mean global cerebral NAGM for all MS patients (without separation on MS subgroups). Similar analysis was repeated for NAWM and cortical thickness.

To examine the correlation between tissue damage in brain and spinal cord, Pearson's correlation analysis was performed between ΔCSA of C1 and ΔR2t* of each cortical region, ΔCSA of C1 and ΔR2t* of each subcortical WM region, and ΔCSA of C1 and thickness of each cortical region.

To establish relationships between MS-related tissue damage in adjacent subcortical WM and cortical GM regions, we applied linear regression analysis to the 44 MS patients using the following equation for each cortical region defined in FreeSurfer (n):

$$\frac{\Delta SubcorticalR2t_n^*}{\Delta MeanSubcorticalR2t^*} = q_n \cdot \frac{\Delta \text{ CorticalR } 2t_n^*}{\Delta \text{Mean Cortical} R2t^*} \quad 4$$

where $MeanR2t^*$ is a mean R2t* measurement for the entire cortical GM or subcortical WM in each MS patient. Equation [4] was applied to establish MS-related tissue damage based on all 44 MS patients without regard to MS subtypes.

Correlations of ΔCSA with EDSS, 25FTW, and 9HPT were assessed using Spearman's rank correlation, since these data were not of Gaussian distribution. Parametric data were

analyzed using Pearson's correlation. False discovery rate (FDR) with the Benjamini-Hochberg procedure was used to correct for multiple testing. After correction, $P < 0.05$ was considered significant.

Results

Examples of GEPCI T1W images, R2t* maps, and MPRAGE images for one healthy control and one MS patient are shown in Fig. 1.

The age range and gender ratio was similar for HC and MS patients (demographic and clinical information presented in Table 1). As expected, the mean EDSS was less severe for the RRMS patients than the progressive patients (Table 1).

Topographic Signatures of CNS Tissue Injury in MS

"Visible" tissue damage (lesions in brain WM and the atrophy of the cortex and the cervical spinal cord) and "invisible" tissue damage (reduced R2t* in cortical NAGM and subcortical NAWM of MS patients) were identified and quantified. Group-wise, R2t* of GM readily distinguished HC from MS patients (Fig. 2). Cortical thickness was not significantly different between HC and MS groups, although trends for reduced thickness were observed in the progressive MS groups (Fig. 2). Decreased (1.96 SD lower than mean value of HC group) R2t* of NAGM was present in 48% of the MS patients compared to decreased cortical thickness in only 9% of the MS patients. Group comparisons based on R2t* of subcortical WM, WM TDL, and cervical spinal cord CSA (Fig. 3) showed significant differences between MS patients and HC. There were no detectable lesions in WM of HC, hence HC TDL = 0. Decreased (1.96 SD lower than mean value of HC group) subcortical WM R2t* was present in 43% of the patients, and decreased CSA was present in 45% of the patients.

Since our measurements in cortical GM and subcortical WM did not show significant differences between MS subtypes, all further analyses were performed for MS patients without separation into MS subgroups. Since there were no significant differences of R2t* and cortical thickness measurement between the left and right hemisphere (see Supporting Information), the values of R2t* and TH in the left and right hemispheres were averaged for corresponding ROIs.

The fitting results for R2t* and Thickness per Eq. [3] are listed in the Supporting Information. Since not all coefficients K_n between the ROIs were statistically significant, for further analysis we used the same coefficients K for all ROIs that were determined by fitting global values of R2t* and Thickness. These coefficients were: 0.0303 (GM R2t*), 0.0211 (subcortical WM R2t*), and –0.0052 (GM thickness). These calculated baseline values were subtracted from the values of individual HC and MS subjects to generate ΔR2t* and ΔThickness. The P-values of the correlations between age and global mean R2t* in GM and subcortical WM, and mean cortical thickness were 0.0006, 0.046, 0.003, respectively.

Not all regions of GM and WM were affected equally. To establish patterns of tissue damage between different cortical and subcortical ROIs, we first performed Pearson's correlation

analysis of ΔR2t* in each NAGM cortical region$\left(\Delta R2t_n^*\right)$ versus mean NAGM cortical AR2t* using data for all 44 MS patients. A similar procedure was performed for cortical thickness and ΔR2t* of subcortical NAWM. Patterns of tissue damage, as determined by r values from correlation analyses, are presented on brain surface maps (Fig. 4). The patterns of tissue damage were similar for NAGM and subcortical NAWM: tissue damage in parietal and occipital cortices reflected best with mean cortical tissue damage. Cortical thickness showed a different pattern than R2t* measurement; changes in temporal cortices showed the strongest correlation with the mean cortex thickness change.

Interrelationships Between MS Tissue Injury in Different Topographic Regions

Figures 2–4 show the presence of tissue damage in spinal cord, GM, and WM in MS patients. To test the hypothesis that the strength of tissue damage in different parts of CNS could be interrelated, thus forming MS-related topographic signatures, we ran a correlation analysis between all the quantitative parameters defining MS tissue damage in spinal cord, NAGM, NAWM, and MS lesions. The sizes of spinal cord at C1, C2, C3, and C4 are highly correlated (Supporting Information: Fig. 1A). Since only one focal MS lesion was noted at the C1 level, CSA of C1 was used to correlate with tissue damage measurement in brain and clinical scores.

CSA at C1, tissue damage in NAGM and NAWM in the brain, and tissue damage load of lesions in the brain showed multiple interrelationships, irrespective of MS clinical subtype (Table 2). Reduced R2t* values in global NAGM and subcortical NAWM were significantly correlated with reduced CSA of C1 (Table 2). In contrast, no significant correlations between reduced CSA at C1 and reduced R2t* of GM or subcortical WM was seen for HC ($P = 0.68$ and 0.88, respectively), suggesting that correlations in MS patients are pathology-related. Similarly, MS patients with smaller CSA also had proportionately thinner global cerebral cortices but no significant correlation was found between C1 CSA and thickness of GM for HC ($P = 0.52$).

In addition to the assessments of relationships between characteristics of the spinal cord and the brain globally (Table 2), specific cortical regions were also examined (Fig. 5). Tissue damage characterized by ΔR2t* of middle temporal, inferior temporal, and inferior parietal cortical regions of NAGM showed the most significant correlations with the C1 spinal cord size. For subcortical NAWM, the ΔR2t* of the middle temporal region demonstrated the greatest correlation with CSA at C1. In contrast, and not unexpectedly, among all 34 cortical regions the thickness of the motor cortex was most correlated with C1 spinal cord size (Fig. 5). Thickness of other cortical regions showed either nonsignificant or weak correlations with C1 CSA (Fig. 5).

Table 2 also shows significant correlations between tissue damage measured by mean R2t* of NAGM and mean R2t* of the subcortical NAWM. To assess the relative severity of tissue damage in adjacent regions of cortical NAGM and subcortical NAWM, linear regression based on all 44 MS patients was performed between a decrease of R2t* in each subcortical NAWM region versus a corresponding cortical NAGM regions (per Eq. [4] in Methods). A slope less than 1 indicates that NAGM R2t* has larger relative reduction than NAWM. With

the exception of the inferior temporal cortex, all NAGM regions showed larger relative changes than NAWM (Fig. 6).

Relationship Between Clinical Test Performance and Tissue Damage in Brain and Spinal Cord in MS

To evaluate the relationships between tissue damage and MS clinical signs, mean ΔR2t* of NAGM and NAWM, mean cortical ΔTh, spinal cord atrophy (ΔCSA at C1), and TDL in brain WM lesions were each assessed for correlations with clinical test results (EDSS, 25FTW, 9HPT, SDMT, and PASAT) (Table 3). Region-wise results are presented in the Supporting Information. ΔCSA at C1 had the most significant correlations with motor-related clinical tests EDSS, 25FTW, and 9HPT (dominant and nondominant hands). Similar correlations with clinical tests were found for C2, C3, and C4 (not shown). Mean ΔR2t* of global cortex showed significant correlation with 9HPT (dominant and nondominant hands) and PASAT. WM Tissue damage load based on R2t* correlated with EDSS, PASAT, and SDMT. In the present 44 patient cohort, gender, age, and MS duration did not correlate with physical impairment scores.

Discussion

In this study we addressed three questions. One was to ask if we could detect “invisible” pathology not recognized by standard clinical MRI (based on “weighted” MRI contrasts) in the CNS of MS patients using a new imaging marker, R2t*. The second related question was to ask whether there existedtopographic signatures of MS pathology (visible and invisible) in CNS common to MS patients. The third question was whether our quantitative tissue damage measurements reflected neurological impairment in MS.

Tissue integrity in the brain cortical NAGM and subcortical NAWM of MS patients was quantified using the GRE MRI signal decay rate constant, R2t*. This parameter (R2t*) is a quantitative measure that has been shown to correlate with tissue cellular density in normal human brain[32] and was decreased in brain areas in concert with the loss of tissue cellular integrity in Alzheimer’s disease.[33] Since previous studies demonstrated reduced R2 values in areas of demyelination in the spinal cord[20] and brain,[12,22] and reduced total R2* has been noted in areas of WM[31] and cortical demyelination,[23,34] we expected that a more tissuespecific parameter R2t* would be reduced by demyelination as well. Indeed, in our cohort MS patients had lower R2t* values in both WM and GM as compared with HC participants. We were able to identify regions of “invisible” tissue damage based on comparison of quantitative R2t* measurements in MS and HC participants. The “visible” part of brain tissue damage was also quantitatively assessed in our study by measuring cortical thickness and a quantitative composite measure of WM damage characterizing both WM lesion volume and tissue damage within the lesions: MS lesion TDL. The cervical spinal cord was assessed by measuring upper cervical cord CSA, reductions which predominantly reflect axon loss.

Since age affects R2t* and reduces cortical thickness, baseline correction was used to account for age effects. For spinal cord, no significant correlation was found between spinal cord CSA and age, height, gender, brain size, and disease duration in our data.

For the first question, tissue damage of various degrees not apparent on standard MRI was present in most MS patients in most parts of the CNS we examined. Significant atrophy was present in the cervical spinal cord and cortical GM, with the motor cortex and temporal cortex showing the most significant volume reductions in the brain. Although most cortical regions were affected in at least some patients, the motor cortex and postcentral cortex demonstrated the greatest decreased of R2t* compared to HC. Brain subcortical WM demonstrated a similar pattern, in accord with the strong correlation between R2t* in GM and subcortical WM. No significant correlation between R2t* of cortical NAGM and cortical thickness was found, which means that R2t* and thickness are two complementary measurements— the latter showing reduction in tissue volume while the former showing loss of remaining tissue integrity. We had hypothesized that tissue quality changes (measured by R2t*) should be evident before atrophy. The difference between cortical thickness of healthy controls and MS patients were not statistically significant, possibly due to the relatively small cohort size. Nevertheless, a decreasing trend of cortical thickness was observed in this study, which is consistent with a recent report showing group differences measured by normalized GM volume in a larger cohort of 206 MS patients.[35] Normalized GM volume was also measured in our study and a similar trend as in Ref. 35 was found (Supporting Information: Fig. 2A). Compared with cortical thickness, R2t* measurement readily differentiated MS patients from HC even within our small cohort size. Since more patients showed a significant decrease in R2t* of the NAGM but not in cortical thickness, we suggest that R2t* is more sensitive to tissue injury than cortical atrophy, and has a potential to be used as a sensitive biomarker for MS-related clinical trials.

To answer the second question, correlations between tissue damage in different parts of the CNS were examined. Tissue damage in the cervical spinal cord (assessed by cord atrophy) significantly correlated with tissue damage in the brain cortical NAGM (assessed by cortical atrophy and reduced R2t*), subcortical NAWM (assessed by reduced R2t*), and WM MS lesions (assessed by R2t*-based TDL). Whereas correlations existed between tissue damage in several different parts of the brain and CSA of cervical cord, the strongest and the most significant correlation was found between atrophy of the spinal cord and the thickness of brain motor cortex. This was not surprising, since these two structures are physically and functionally linked, with axons from motor cortical neurons extending through the cervical cord; when a motor neuron dies, its axons degenerate.

Another interrelationship (cortical GM – subcortical WM) was identified by strong correlations between tissue damage in the adjacent regions of cortical GM and subcortical WM. Table 2 shows that decreases of R2t* in cortical NAGM and subcortical NAWM were highly correlated. We further examined the relative severity of tissue damage between NAGM and NAWM. Our measurements show that R2t* changes in GM were relatively bigger in most ROIs than in adjacent WM ROIs, which may suggest that tissue damage is relatively more severe in cortical NAGM compared with subcortical NAWM. This interpretation would be in accord with a previous study that found the percentage of demyelinated area was significantly higher in cerebral cortex than in WM of MS patients.[36]

It was also notable that the reduced CSA of the cervical spinal cord significantly correlated with “invisible” tissue damage (assessed by R2t*) in the primary motor cortex, and temporal

and inferior parietal cortices. Interestingly, correlations with cord CSA were noted even for regions of cortex, such as occipital, that do not directly link to the spinal cord. Although the biological meaning of these correlations is not obvious, they did not exist in HC, indicating that they are pathology-related. The significant associations between visible and invisible tissue damage in all parts of the CNS further support the concept of MS as a global disease of the CNS.

Certain regions of the CNS are known to be more frequently affected by MS. In particular, these are periventricular areas, juxtacortical white matter, corpus callosum, cortical gray matter, optic nerves, medial longitudinal fasciculus, cerebellar tracts, and the cervical spinal cord[37]. Although the current study did not examine the tissue damage in every region of the CNS, our data still showed tissue damage patterns in the CNS of the 44 MS patients in our cohort. Whether these patterns are generally common to MS patients will need confirmation in larger and different MS patient cohorts. These data are also consistent with recent reports of correlations between spinal cord MRI measurement and retinal layers in MS,[38] and associations between deep gray matter tissue damage and degeneration in cortex and spinal cord.[39]

To address the third question, we examined relationships of tissue damage assessed by R2t* and cortical thickness in different parts of the CNS and C1 CSA with neurological function. A composite measure for TDL based on ΔR2t* values in the WM lesions correlated with EDSS, but to a lesser degree than cervical CSA. Of all our imaging measures, the cervical cord CSA correlated best with physical impairment defined by EDSS and 25FTW tests, in accord with several previous studies.[40]

Not surprising, no correlation was found in this study between cognitive tests (SDMT and PASAT) and spinal cord cross-sectional size. On the other hand, ΔR2t* values of the entire cortical GM and several specific cortical regions correlated significantly with SDMT and PASAT scores. These correlations with cognitive test results were more widespread and greater than for cortical thickness, indicating that ΔR2t* is more sensitive to tissue damage. The region-wise analysis showed the correlation between GM, subcortical WM R2t*, and 9HPT (dominant and nondominant) were similar. However, subcortical WM R2t* showed stronger correlation with cognitive tests compared with GM R2t*.

Based on these findings we can hypothesize that R2t* alterations might be an early indicator of MS pathology, detectable at a time when atrophy is not apparent. In the future, we plan to create a model incorporating R2t* and other imaging parameters, to explain concurrent physical impairment status with the ultimate goal of predicting the future MS course.

In this study we have not reported tissue-specific R2t* measurements in the upper cervical spinal cord due to technical issues related to low SNR in our data in the spinal cord. RF coils covering both brain and spinal cord would allow simultaneous R2t* mapping in the brain and spinal cord without increased scanning time. Improvement in RF coil design could potentially allow R2t* mapping of small CNS structures (eg, optical nerve) that was not visible with our current design. Generating R2t* maps on the scanner requires computer power that is currently not available from manufacturers and therefore we analyzed data

offline. While timing is crucial for diagnostic acute medical conditions (eg, stroke, heart attack, etc.), delays with generating diagnostic images based on R2t* metric can be tolerated for chronic conditions like MS. Future improvement of the time to generate usable results will likely be resolved with the development of more powerful computers and using cloud computing.

In conclusion, we report the novel finding that a quantitative measure of MS tissue damage based on the tissue cellular specific transverse relaxation rate constant, R2t*, can sensitively detect MS-related pathology in cortical NAGM, subcortical NAWM, and WM lesions. The method demonstrated tissue damage patterns in the CNS of the MS cohort. Our data shed light on the interrelationships of damage throughout the brain and cervical spinal cord, while supporting the idea of MS as a global CNS disease. Our results showed that, while spinal cord CSA is a reliable marker for changes in motor functions, the reduction in the R2t* of GM and WM is a reliable indicator of cognitive dysfunction.

Supplementary Material

Refer to Web version on PubMed Central for supplementary material.

Acknowledgments

Contract grant sponsor: University of Missouri Columbia; Contract grant number: SCIR 14–01; Contract grant sponsor: Conrad N. Hilton Foundation; contract grant number: 20140257; Contract grant sponsor: National MS Society USA; Contract grant number: NMSS RG 4463A182; Contract grant sponsor: NIH; Contract grant number: R01 AG054513. Anne H. Cross and Dmitriy A. Yablonskiy hold a Marilyn Hilton Award for Innovation in MS Research from the Conrad N. Hilton Foundation. Jie Wen was a Fellow of the National MS Society USA during these studies. The authors thank Drs. Joseph Ackerman and Salim Chahin for helpful discussions and Dr. Amber Salter for advice on statistical measures.

References

1. Traboulsee AL, Li DK. The role of MRI in the diagnosis of multiple sclerosis. Adv Neurol 2006;98:125–146. [PubMed: 16400831]
2. Sormani MP, Bruzzi P, Beckmann K, et al. MRI metrics as surrogate endpoints for EDSS progression in SPMS patients treated with IFN beta-1b. Neurology 2003;60:1462–1466. [PubMed: 12743232]
3. Bermel RA, You X, Foulds P, et al. Predictors of long-term outcome in multiple sclerosis patients treated with interferon beta. Ann Neurol 2013; 73:95–103. [PubMed: 23378325]
4. Naismith RT, Cross AH. Multiple sclerosis and black holes: connecting the pixels. Arch Neurol 2005;62:1666–1668. [PubMed: 16286537]
5. Harel A, Ceccarelli A, Farrell C, et al. Phase-sensitive inversion-recovery MRI improves longitudinal cortical lesion detection in progressive MS. PLoS One 2016;11:e0152180. [PubMed: 27002529]
6. Fisher E, Chang A, Fox RJ, et al. Imaging correlates of axonal swelling in chronic multiple sclerosis brains. Ann Neurol 2007;62:219–228. [PubMed: 17427920]
7. Bot JC, Barkhof F, Polman CH, et al. Spinal cord abnormalities in recently diagnosed MS patients: added value of spinal MRI examination. Neurology 2004;62:226–233. [PubMed: 14745058]
8. Lukas C, Sombekke MH, Bellenberg B, et al. Relevance of spinal cord abnormalities to clinical disability in multiple sclerosis: MR imaging findings in a large cohort of patients. Radiology 2013;269:542–552. [PubMed: 23737540]
9. Derakhshan M, Caramanos Z, Narayanan S, Arnold DL, Louis Collins D. Surface-based analysis reveals regions of reduced cortical magnetization transfer ratio in patients with multiple sclerosis: a

proposed method for imaging subpial demyelination. Hum Brain Mapp 2014;35:3402–3413. [PubMed: 24356893]

10. Hulst HE, Steenwijk MD, Versteeg A, et al. Cognitive impairment in MS: impact of white matter integrity, gray matter volume, and lesions. Neurology 2013;80:1025–1032. [PubMed: 23468546]
11. Kolind SH, Deoni SC. Rapid three-dimensional multicomponent relaxation imaging of the cervical spinal cord. Magn Reson Med 2011;65: 551–556. [PubMed: 20882672]
12. MacKay A, Whittall K, Adler J, Li D, Paty D, Graeb D. In vivo visualization of myelin water in brain by magnetic resonance. Magn Reson Med 1994; 31:673–677. [PubMed: 8057820]
13. Mainero C, Louapre C, Govindarajan ST, et al. A gradient in cortical pathology in multiple sclerosis by in vivo quantitative 7 T imaging. Brain 2015;138:932–845. [PubMed: 25681411]
14. Ge Y Multiple sclerosis: the role of MR imaging. AJNR Am J Neuroradiol 2006;27:1165–1176. [PubMed: 16775258]
15. Ulrich X, Yablonskiy DA. Separation of cellular and BOLD contributions to T2* signal relaxation. Magn Reson Med 2016;75:606–615. [PubMed: 25754288]
16. Luo J, Jagadeesan BD, Cross AH, Yablonskiy DA. gradient echo plural contrast imaging — signal model and derived contrasts: T2*, T1, phase, SWI,T1f, FST2* and T2*-SWI. NeuroImage 2012;60:1073–1082. [PubMed: 22305993]
17. Ogawa S, Lee TM, Kay AR, Tank DW. Brain magnetic resonance imaging with contrast dependent on blood oxygenation. Proc Natl Acad Sci U S A 1990;87:9868–9872. [PubMed: 2124706]
18. Yablonskiy DA, Sukstanskii AL, Luo J, Wang X. Voxel spread function method for correction of magnetic field inhomogeneity effects in quantitative gradient-echo-based MRI. Magn Reson Med 2013;70:1283–1292. [PubMed: 23233445]
19. Wen J, Cross AH, Yablonskiy DA. On the role of physiological fluctuations in quantitative gradient echo MRI: implications for GEPCI, QSM, and SWI. Magn Reson Med 2015;73:195–203. [PubMed: 24482009]
20. Bot JC, Blezer EL, Kamphorst W, et al. The spinal cord in multiple sclerosis: relationship of high-spatial-resolution quantitative MR imaging findings to histopathologic results. Radiology 2004;233:531–540. [PubMed: 15385682]
21. Laule C, Kozlowski P, Leung E, Li DK, Mackay AL, Moore GR. Myelin water imaging of multiple sclerosis at 7 T: correlations with histopathol- ogy. NeuroImage 2008;40:1575–1580. [PubMed: 18321730]
22. Seewann A, Vrenken H, van der Valk P, et al. Diffusely abnormal white matter in chronic multiple sclerosis: imaging and histopathologic analysis. Arch Neurol 2009;66:601–669. [PubMed: 19433660]
23. Patel KR, Luo J, Alvarez E, et al. Detection of cortical lesions in multiple sclerosis: A new imaging approach. Mult Scler J Exp Transl Clin 2015;1: 2055217315606465. [PubMed: 28607704]
24. Fischer JS, Rudick RA, Cutter GR, Reingold SC. The Multiple Sclerosis Functional Composite Measure (MSFC): an integrated approach to MS clinical outcome assessment. National MS Society Clinical Outcomes Assessment Task Force. Mult Scler 1999;5:244–250. [PubMed: 10467383]
25. Mugler JP, 3rd, Brookeman JR. Three-dimensional magnetization- prepared rapid gradient-echo imaging (3D MP RAGE). Magn Reson Med 1990;15:152–157. [PubMed: 2374495]
26. Yablonskiy DA. Quantitation of intrinsic magnetic susceptibility-related effects in a tissue matrix. Phantom study. Magn Reson Med 1998;39: 417–428. [PubMed: 9498598]
27. Yablonskiy DA, Haacke EM. Theory of NMR signal behavior in magnetically inhomogeneous tissues: the static dephasing regime. Magn Reson Med 1994;32:749–63. [PubMed: 7869897]
28. De Leener B, Levy S, Dupont SM, et al. SCT: Spinal cord Toolbox, an open-source software for processing spinal cord MRI data. NeuroImage 2017;145:24–43. [PubMed: 27720818]
29. Shiee N, Bazin PL, Ozturk A, Reich DS, Calabresi PA, Pham DL. A topology-preserving approach to the segmentation of brain images with multiple sclerosis lesions. NeuroImage 2010;49:1524–1535. [PubMed: 19766196]
30. McAuliffe MJ, Lalonde FM, McGarry D, Gandler W, Csaky K, Trus BL. Medical image processing, analysis and visualization in clinical research. Proceedings 14th IEEE Symposium on Computer-Based Medical Systems, 2001 CBMS 2001 2001; p 381–386.

31. Sati P, Cross AH, Luo J, Hildebolt CF, Yablonskiy DA. In vivo quantitative evaluation of brain tissue damage in multiple sclerosis using gradient echo plural contrast imaging technique. NeuroImage 2010;51: 1089–1097. [PubMed: 20338247]
32. Zhao Y, Wen J, Cross AH, Yablonskiy DA. On the relationship between cellular and hemodynamic properties of the human brain cortex throughout adult lifespan. NeuroImage 2016;133:417–429. [PubMed: 26997360]
33. Zhao Y, Raichle ME, Wen J, et al. In vivo detection of microstructural correlates of brain pathology in preclinical and early Alzheimer disease with magnetic resonance imaging. NeuroImage 2017;148:296–304. [PubMed: 27989773]
34. Wen J, Yablonskiy DA, Luo J, Lancia S, Hildebolt C, Cross AH. Detection and quantification of regional cortical gray matter damage in multiple sclerosis utilizing gradient echo MRI. NeuroImage Clin 2015;9:164–175. [PubMed: 27330979]
35. Steenwijk MD, Geurts JJ, Daams M, et al. Cortical atrophy patterns in multiple sclerosis are non-random and clinically relevant. Brain 2016;139: 115–126. [PubMed: 26637488]
36. Bo L, Vedeler CA, Nyland HI, Trapp BD, Mork SJ. Subpial demyelination in the cerebral cortex of multiple sclerosis patients. J Neuropathol Exp Neurol 2003;62:723–732. [PubMed: 12901699]
37. Guo YF, Lucchinetti C. Taking a microscopic look at multiple sclerosis 2016; p:65–88. New York: Oxford University Press, Inc.
38. Oh J, Sotirchos ES, Saidha S, et al. Relationships between quantitative spinal cord MRI and retinal layers in multiple sclerosis. Neurology 2015; 84:720–728. [PubMed: 25609766]
39. Ruggieri S, Petracca M, Miller A, et al. Association of deep gray matter damage with cortical and spinal cord degeneration in primary progressive multiple sclerosis. JAMA Neurol 2015;72:1466–1474. [PubMed: 26457955]
40. Losseff NA, Webb SL, O'Riordan JI, et al. Spinal cord atrophy and disability in multiple sclerosis. A new reproducible and sensitive MRI method with potentialtomonitordiseaseprogression.Brain1996;119(Pt3):701–708. [PubMed: 8673483]

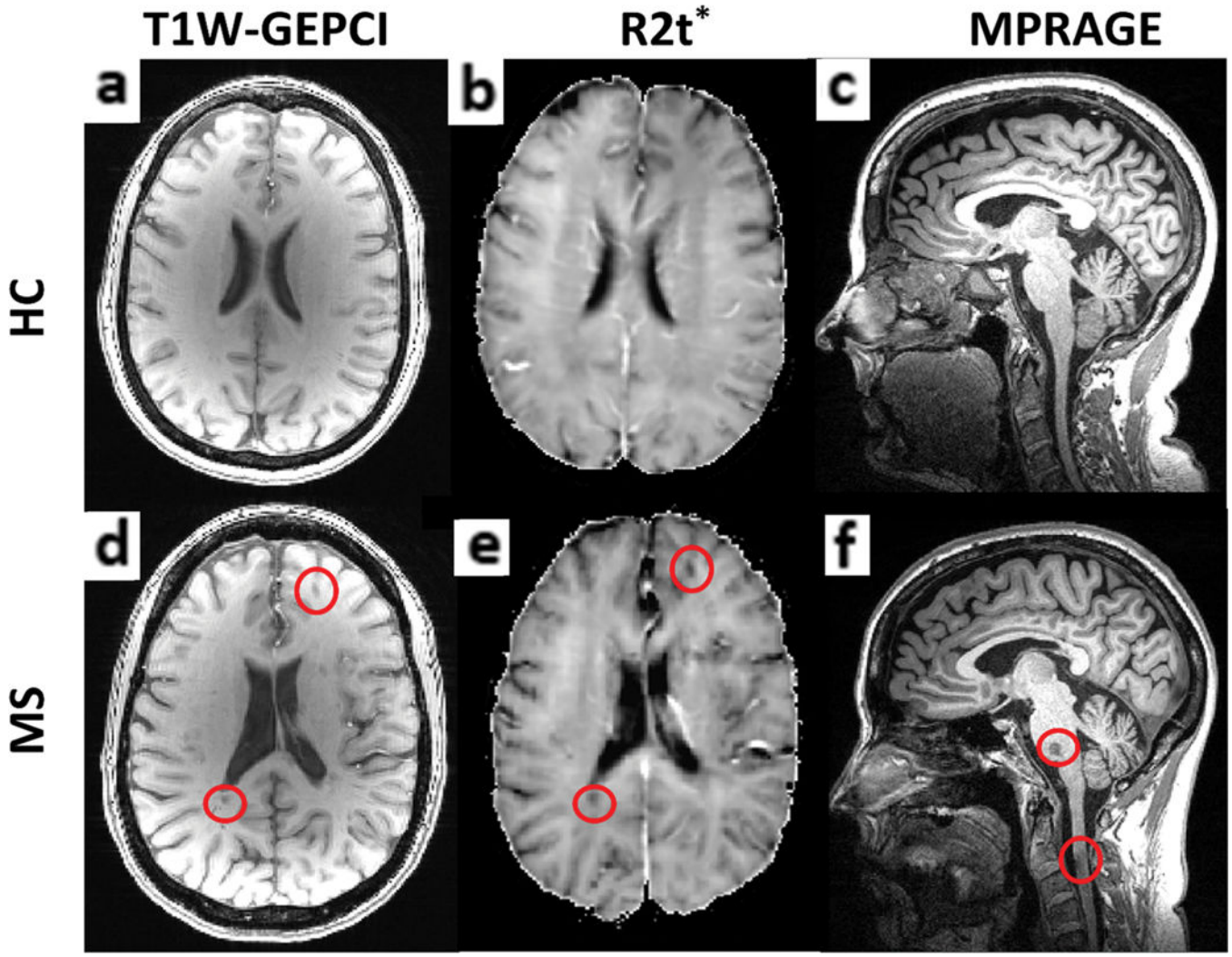

FIGURE 1: Examples of axial GEPCI Tl-weighted images and R2t* maps are shown along with sagittal MPRAGE images of one healthy control

(a–c) and one MS patient **(d–f).** Images shown come from similarly aged female (58 and 55 years old) HC and MS patients. In the MS patient, two cerebral lesions, one pontine lesion, and one spinal cord lesion at the C2–3 level are outlined by red circles.

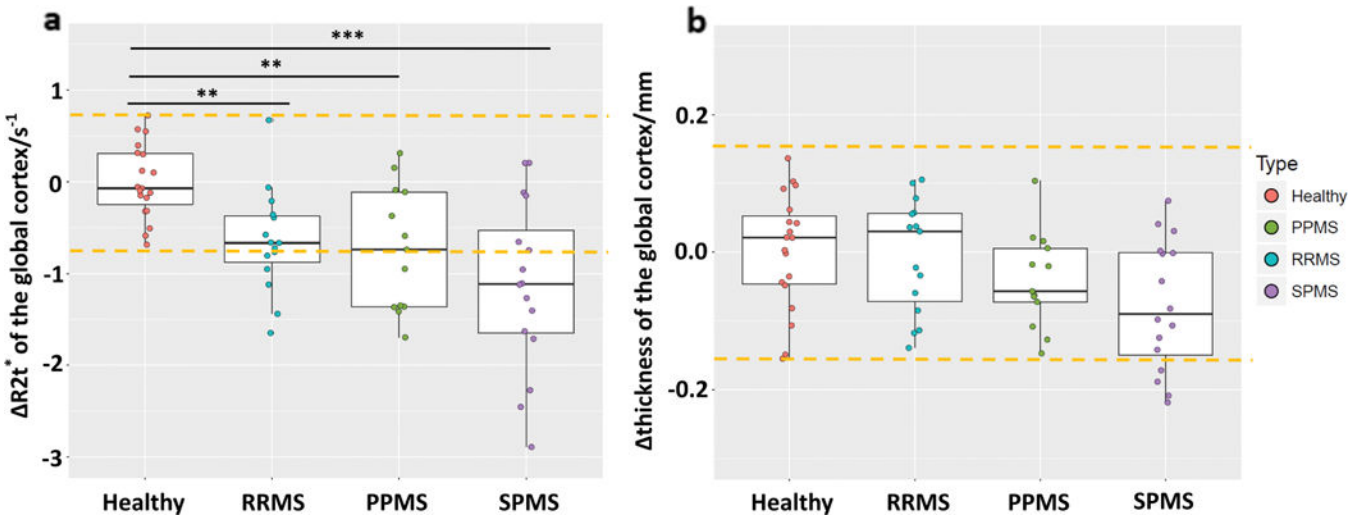

FIGURE 2: Group comparisons based on the mean global cortical R2t*

(a) and mean global cortical thickness **(b)**. Cortical R2t* performs better than thickness in distinguishing MS patients from HC on both the group and individual levels. At the individual level, decreased (1.96 SD of HC group lower than mean value of HC group) R2t* was present in 48% of MS patients compared to decreased cortical thickness in only 9%. Yellow dashed lines indicate 1.96 SD of HC group lower/higher than mean value of HC group. Boxes represent the interquartile ranges; the horizontal lines within the boxes indicate median values, points are median values of individual patients. ***$P < 0.001$, **$P < 0.01$, *$P < 0.05$. All P values were determined after adjusting for multiple comparisons using the FDR.

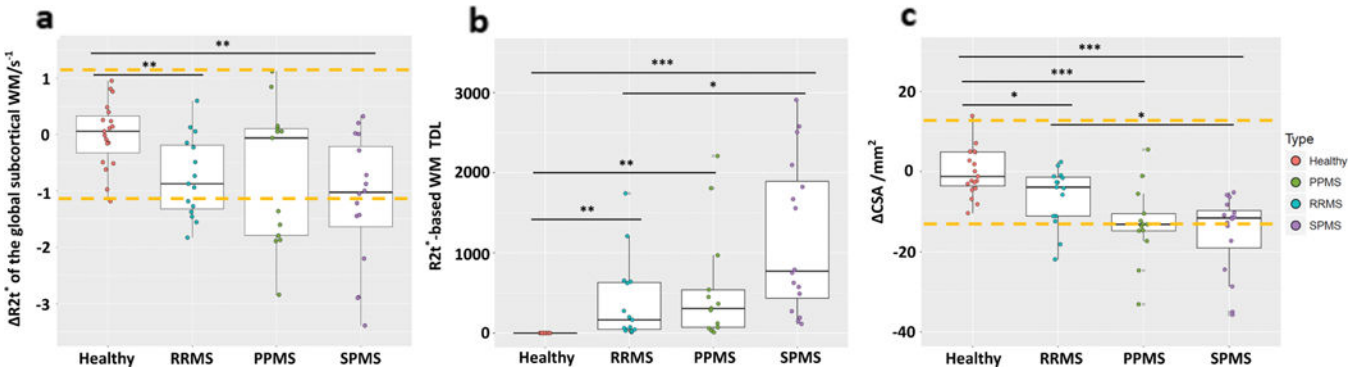

FIGURE 3: Group comparisons based on the mean global subcortical WM R2t*

(a), WM TDL **(b)**, and mean CSA **(c)**. Most MS patients showed decreased R2t* in subcortical NAWM and mean spinal cord CSA (averaged spinal cord cross-sectional area from C1 to C4). Yellow dashed lines indicate 1.96 SD of HC group lower/higher than mean value of HC group. Boxes represent the interquartile ranges; the horizontal lines within the boxes indicate median values, points are median values of individual patients. ***$P < 0.001$, **$P < 0.01$, *$P < 0.05$. All P values were determined after adjusting for multiple comparisons using the FDR.

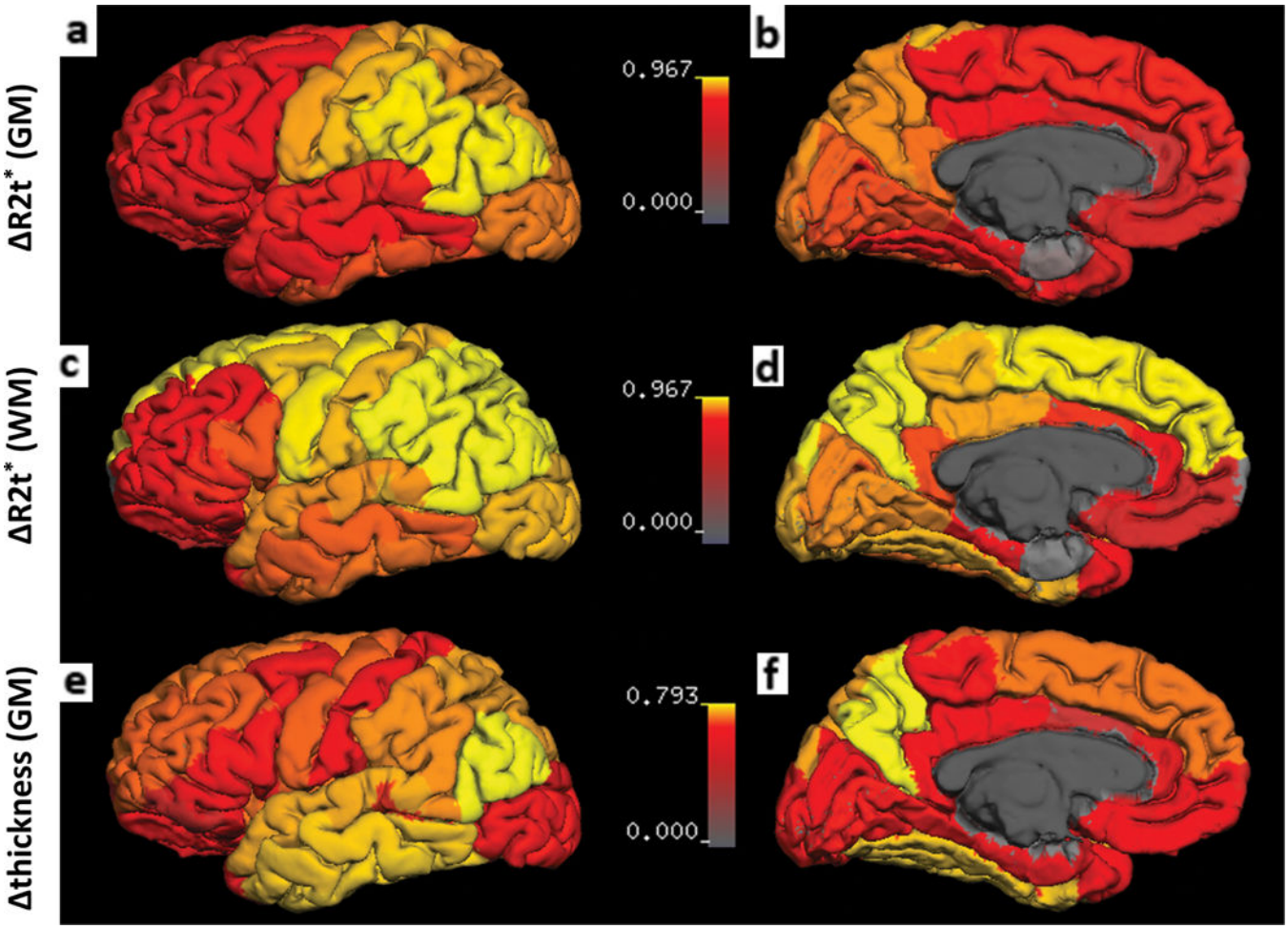

FIGURE 4: Topographic signatures of tissue damage in NAGM and NAWM.

(a,b) *r* value from Pearson's correlation analysis between **Δ**R2t* of each cortical region (*n*) vs. **Δ**R2t* of the mean global cerebral NAGM for all MS patients (without separation on MS subgroups) are mapped on the cortical surface. Decrease of R2t* in the motor and postcentral cortex were most reflective of the mean global cortical decrease of R2t*. **(c,d)** The same analysis for subcortical NAWM. The pattern of change in **Δ**R2t* of NAWM was similar to NAGM. **(e,f)** The same analysis for cortical GM **Δ**Thickness. Decrease of thickness in the temporal lobe correlated most with the mean decrease of thickness in global cortex. The surface of the cortex was generated by FreeSurfer. Deep GM structures, WM, and ventricles were excluded. Color bars represent r value from Pearson's correlation analysis.

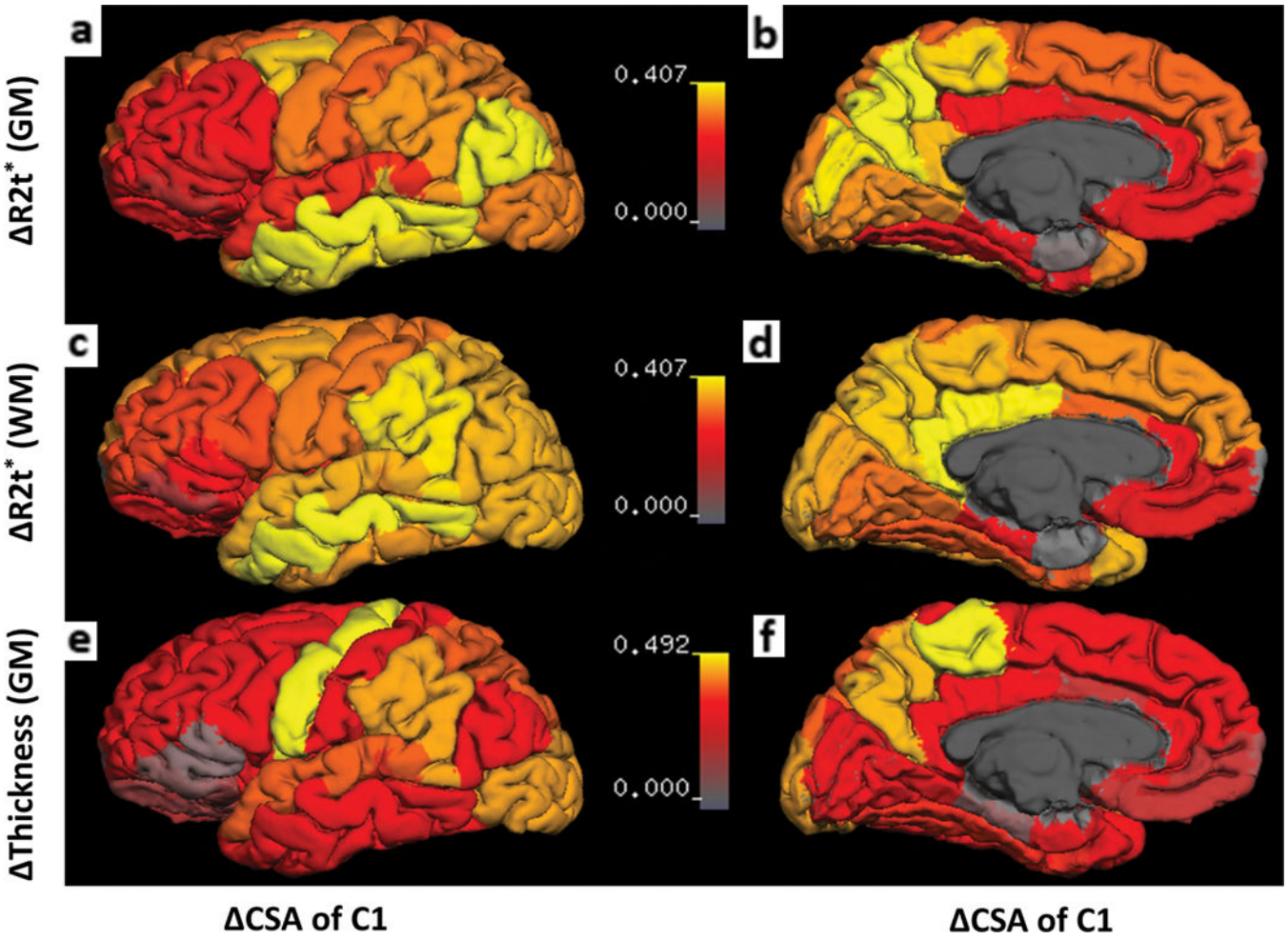

FIGURE 5: Results of the correlation analyses between tissue damage in the brain and the spinal cord based on all 44 MS patients. All images show the *r* values of the Pearson's correlation coefficient mapped on the cortical surface.

(a,b) Correlation between **Δ**CSA of C1 and **Δ**R2t* of cortical GM. The primary motor cortex and the somatosensory cortex showed moderate correlations with C1 **Δ**CSA. **(c,d)** Correlation between **Δ**CSA of C1 and **Δ**R2t* in subcortical WM regions. The middle temporal subcortical WM demonstrated the highest correlations with C1 **Δ**CSA. **(e,f)** Correlation between **Δ**CSA of C1 and **Δ**Thickness in cortical regions. The primary motor cortex showed the strongest correlation with C1 ACSA, while other regions either showed very weak or no significant correlations. The surface of the cortex was generated by FreeSurfer. Deep GM structures, WM, and ventricles were excluded. Color bars represent *r* values.

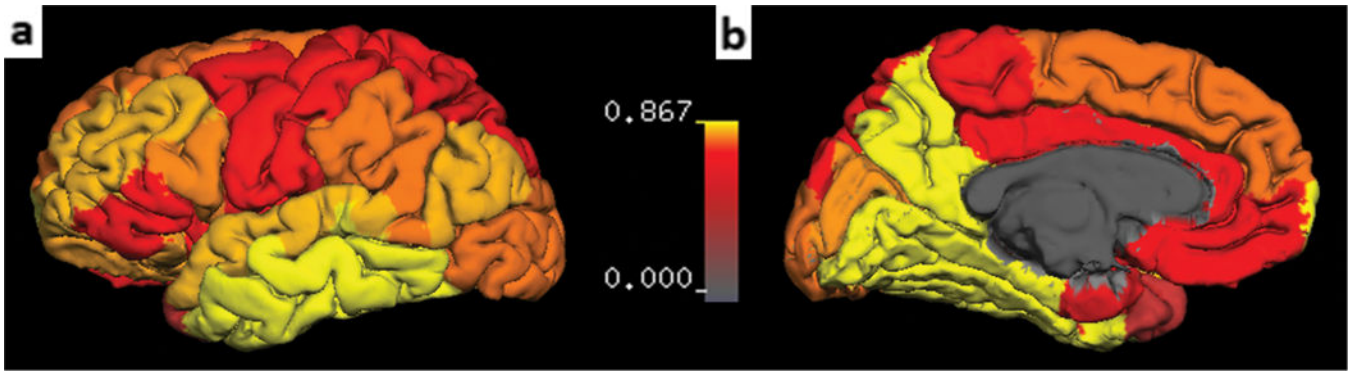

FIGURE 6:

Slopes of linear regressions between ΔR2t* of adjacent subcortical NAWM vs. ΔR2t* of matched cortical NAGM regions (parameter q_n in Eq. 6). Data are based on all 44 MS patients. Images represent parameter q_n projected on the cortical surface generated by FreeSurfer. Deep GM structures, WM, and ventricles were excluded. Color bar represents q_n values.

TABLE 1.

Summary of Subject Demographic and Clinical Information

			MS		
		Healthy control	**RRMS**	**PPMS**	**SPMS**
Number		19	15	13	16
Mean age ± SD (years)		46.7 + 13.6 (23–76)	49.4 ± 10.4 (32–60)	55.2 ± 10.2 (37–74)	59.2 ± 9.3 (45–75)
Female/male		14/5	12/3	8/5	10/6
Disease duration (years)		n/a	15.8 ± 7.7	15.8 ± 9.6	21.1 ± 10.0
EDSS mean ± SD (range)		n/a	2.6 ± 1.3 (1–6)	5.7 ± 1.1 (4.0–6.5)	5.6 ± 1.5 (3.5–8)
25FTW mean ± SD (range)		n/a	5.0 ± 1.9 (2.7–11)	11.8 ± 8.9 (3.9–30)	11.0 ± 4.5 (5.7–17.1)
9HPT mean ± SD (range)	Dominant	n/a	22.7 ± 5.6 (15.2–36.7)	28 ± 6.9 (18.3–39.8)	30.2 ± 7.9 (20.3–46.2)
	Nondominant	n/a	22.6 ± 5.2 (16.3–32.5)	28.9 ± 8.6 (18.6–45.3)	31.8 ± 7.7 (23.7–47.2)
SDMT mean ± SD (range)		n/a	52.7 ± 13.0 (10–65)	52.6 ± 9.6 (39–72)	41.6 ± 13.9 (11–62)
3 sec PASAT mean ± SD C(range)		n/a	43.9 ± 10.9 (27–55)	49 ± 10.4 (28–60)	41.6 ± 11.9 (21–58)

EDSS, Expanded Disability Status Scale; 25FTW, 25-foot timed walk (seconds); 9HPT, nine-hole peg test (seconds). For the 25FTW, four MS patients could not finish the test. One MS patient could not finish the 9HPT (dominant hand) and three MS patients could not finish the 9HPT (nondominant hand).

TABLE 2.

Summary of Correlations Between Different Tissue Damage Measurements in CNS for 44 MS Patients

	ΔR2t* of global NAGM	**ΔR2t* of global subcortical NAWM**	**ΔTh of global NAGM**	**Brain WMTDL**
ΔCSA of C1	* $r = 0.39$	* $r = 0.38$	** $r = 0.43$	$P = 0.13$ $r = -0.25$
ΔR2t* of global NAGM		*** $r = 0.80$	$P = 0.61$ $r = 0.079$	$P = 0.16$ $r = -0.31$
ΔR2t* of global Ćsubcortical NAWM			$P = 0.29$ r = 0.18	*** $r = -0.55$
ΔTh of global NAGM				** $r = -0.46$

*** $P < 0.001$,

** $P < 0.01$,

* $P < 0.05$.

All the *P* values presented after correction for multiple comparison via false discovery rate.

TABLE 3.

Summary of Clinical Test Correlations With Spinal Cord Size at C1, Mean R2t* of Global Cortex, Mean R2t* of Subcortical WM, Mean Thickness of Global Cortex, and Brain White Matter Tissue Damage Load for the 44 MS Subjects

	ΔCSA at C1		Mean ΔR2t* Ćof cortex		Mean ΔR2t* of subcortical wm		Mean ΔTh of cortex		TDL	
	r	***P***	***r***	***P***	***r***	***P***	***r***	***P***	***r***	***P***
EDSS	−0.61	***	−0.12	0.51	−0.080	0.65	−0.46	**	0.36	*
25FTW	−0.62	***	−0.19	0.27	−0.16	0.36	−0.41	*	0.29	0.085
9HPT Ć(Dominant)	0.47	**	0.37	*	0.21	0.22	0.26	0.14	−0.25	0.14
9HPT Ć(Nondominant)	0.34	*	0.53	**	0.42	*	0.21	0.16	−0.32	0.056
PASAT	0.051	0.77	0.45	**	0.46	**	0.016	0.92	−0.39	*
SDMT	0.14	0.42	0.30	0.051	0.39	*	0.26	0.23	−0.44	*

r is the Pearson correlation coefficient, all the *P* values presented after correction for multiple comparison via false discovery rate.

*** $P < 0.001$,

** $P < 0.01$,

* $P < 0.05$.